

ANALYTICAL FORMULATION OF THE RADIATION OF SOUND FROM A RECTANGULAR LINED DUCT

Sid-Ali Meslioui

Aiolos Engineering Corporation
51 Constellation Court, Toronto, Ontario, M9W 1K4, Canada.

Jérémie Voix

SUMMARY

This paper deals with the radiation of sound from the open-end of a flanged rectangular lined duct. The duct model consists of a semi-infinite rectangular duct with a lined section of length L . The efficiency of the acoustic treatment for the radiated sound is evaluated by comparing the total power radiated from a duct with and without the lined section. This procedure also allows evaluation of the directivity patterns. The transmitted modal coefficients at the impedance discontinuity junction for a propagating mode (plane wave or higher order mode), incident from the rigid duct, are calculated. Simple analytical tools to predict the radiation of sound have been developed by using the "baffled membrane" approximation method. This model cannot handle reflections from the end, nor radiation to the back, nor an eventual outside flow. However, it is well adapted to the case of a lined duct treated with an arbitrary acoustic impedance, where an exact solution for even a two-dimensional duct is difficult. This method can be applied to turbofan noise and to HVAC systems for possible altering of the radiation pattern by either modifying the radiation field or the types of propagating modes.

SOMMAIRE

Nous présentons ici un modèle simplifié du rayonnement acoustique par l'extrémité d'un conduit droit à section rectangulaire dont seule la partie terminale est traitée par un revêtement absorbant sur une longueur donnée L . Lorsqu'une onde acoustique incidente, constituée d'un mode de propagation donné, arrive sur la portion traitée, il se forme une onde transmise et une onde réfléchi, toutes deux combinaisons de modes de propagation. Les modes de l'onde transmise sont atténués puisque les nombres d'ondes associés sont complexes. S'ils atteignent l'extrémité du conduit en conservant une amplitude suffisante, ils rayonnent à l'extérieur. Dans un premier temps, on calcule les coefficients modaux des modes transmis, puis le rayonnement acoustique par l'extrémité. Cependant, le modèle proposé ne prend en compte ni les réflexions, ni le rayonnement vers l'arrière, ni un éventuel écoulement du milieu extérieur. En revanche, il fournit des résultats simples à exploiter et se prête donc parfaitement à une étude paramétrique. De plus, il est parfaitement adapté au cas d'un conduit avec parois absorbantes, alors que la prise en compte d'une impédance de paroi induit des complications considérables dans la solution analytique exacte, même en configuration bidimensionnelle. Finalement, ce modèle a l'avantage de fournir un outil de calcul prévisionnel du rayonnement acoustique par l'extrémité d'un conduit bafflé.

1. INTRODUCTION

In general, a propagating acoustic mode in a duct (plane wave or higher order mode) suffers diffraction at the exit plane of the duct. This phenomena results in both reflected and incident waves in the duct, as well as the radiation of the sound to the outside. The description of the phenomena in the near field is quite complicated, and in general, greater interest is given to the radiated sound in the far field.

The initial studies on the radiation of sound from an infinite

rectangular flanged duct were conducted by Rayleigh [1]. The radiated sound was calculated from the known end section acoustic velocity by using the so-called "Rayleigh Integral." This approximation is also known as "baffled membrane method." Many later studies are based on this model.

The exact solution of the radiation problem, for the fundamental mode, from the end of a semi-infinite circular duct was developed by Levine and Schwinger [2], who applied the Wiener-Hopf technique [3] to solve the integral

equation. The study showed that the plane wave reflection coefficient tends to zero at high frequencies which means that an approximate solution can thus be obtained by neglecting the reflection from the end at high frequencies. Later, Tyler and Sofrin [4] proposed a similar solution for the case of a rectangular or an annular duct for any incident mode. They found out that, in the case of higher order modes, the reflection coefficients need to be considered only near the cut-off frequencies of the modes while it tends to zero quickly above these frequencies (Morfeý [5] and Homicz et al. [6]). The case of a lined duct with a known acoustic impedance was solved by Zorumski [7]. Later, Lansing et al. [8] studied the effect of the impedance of the duct walls on the transmission-reflection coefficients and on the radiation from the end of a baffled duct.

Koch [9] used the Wiener-Hopf technique to study the effect of a finite layer of an acoustic material, in a two dimensional semi-infinite duct, on the propagation and radiation of modes. He showed that the attenuation for a given mode is effective only around its cut-off frequency. However, the acoustic field has considerably changed because of the conversion of the modes due to the presence of the liner. Johnston and Ogimoto [10] also used the Wiener-Hopf technique to study the radiation of sound from the end of a finite cylinder containing uniform flow. Their method had to resort to many numerical approximations due to complicated analytical developments. Finally, Candel [11] developed analytical expression to calculate the radiation of acoustic modes from the end of a duct with uniform mean flow. He applied Fraunhofer approximation to the Kirchhoff formulation (formulation similar to that of the baffled membrane). The results were similar those obtained by Wiener-Hopf techniques.

The above studies mainly dealt with semi-infinite duct with simple geometry. The difficulties arise when the geometry or the shape of the duct is no longer straight, where only numerical methods (Finite Element or Boundary Element Methods) seem to be useful. These numerical methods, Kagawa et al. [12], and Wu and Lee [13], can be used to solve for ducts of arbitrary cross-sections and with finite length. However, these methods are frequency dependent and require a long computational time. Finally, Hamdi [14, 15] developed a method to predict the noise radiated from finite length ducts with arbitrary shape. The computation of the internal and external acoustic field is based upon a new variational formulation of the integral equations.

It is seen that the exact solution for the radiation of sound from an open duct of arbitrary shape or for a lined duct is not possible. This paper presents a simple method to predict the radiation of sound from a semi-infinite rectangular lined duct. The acoustic treatment is over length L , near the open end. This model, even though complicated due to the presence of the lined section, seems to provide more realistic results compared to the cases of fully lined and

unlined ducts to determine the attenuation provided by the liner. Furthermore, this model will be of great use because of its simple formulation in turbofan noise and HVAC systems design.

The efficiency of the acoustic treatment for the radiated sound is evaluated by comparing the total power radiated from a duct with and without the lined section. This procedure can also be used to study the directivity patterns. However, this model is not suitable to evaluate end reflections or ducts with mean flow.

The presence of a lined section induces a discontinuity problem which is solved in the first part. The modal coefficients of the transmitted modes are calculated from a matrix system which depends on the eigenvalues of the duct modes.

The second part deals with the radiation problem. A comparison between an exact solution obtained by using Wiener-Hopf techniques, Candel [11,18], and the approximate solution based on the baffled membrane method for the radiation of sound from a two semi-infinite parallel plates, is also discussed. This comparison provides a validation of the model elaborated in the last section. Furthermore, analytical expressions are also given to calculate the radiation of sound from the end of the duct.

2. SOUND PROPAGATION IN DUCT WITH DISCONTINUITY OF IMPEDANCE

Sound propagation in a flanged rectangular duct treated with acoustic lining over a length L near the flanged end is analyzed in this section. The duct and the coordinate system are shown in Figure 1. The first section of the duct (section I) has rigid walls; the second section (section II) has its all four walls treated with an acoustic liners with known normal acoustic impedance. Let us now consider an acoustic mode (m_0, n_0) incident from the rigid section I with an amplitude $A_{m_0 n_0}$. The acoustic mode, at the junction between the lined and unlined sections of the duct, is partly transmitted into the lined section as a series of modes with complex amplitudes \hat{A}_{qp} and partly reflected back into the rigid section I with complex modal amplitudes \hat{B}_{mm} . The acoustic energy in the incident mode is thus partially transmitted into the lined section and partially reflected back. The determination of the amplitudes of the transmitted modes is described in section 2.2.

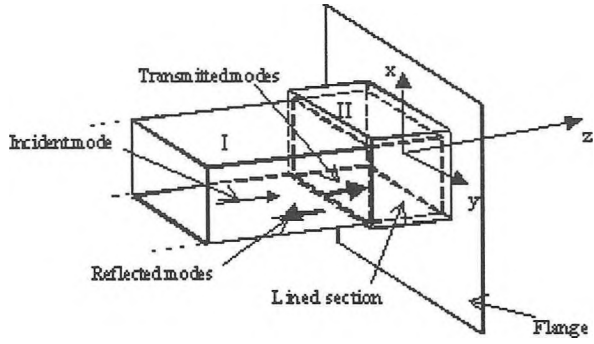


Figure 1-a: Flanged rectangular duct with an acoustically lined end section

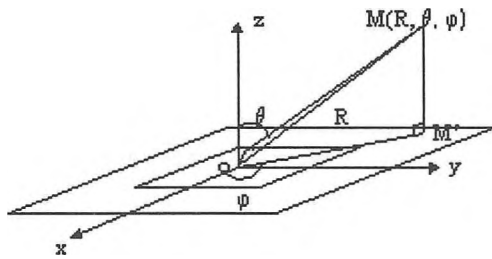


Figure 1-b: Radiation system coordinates

2.1 Basic Equations

The acoustic field inside the duct is determined by the Helmholtz equation

$$\Delta P + k^2 P = 0 \quad (1)$$

where P is the acoustic pressure, $k = \omega/c_0$ is the wave number, ω the angular frequency and ρ , c_0 are the ambient density and speed of sound respectively. The sidewall boundary conditions are

- In section I: $\frac{\partial P}{\partial \tilde{\mathbf{n}}} = 0$
at $x = \pm l_x/2$; $y = \pm l_y/2$ (2)

- In section II: $\frac{\partial P}{\partial \tilde{\mathbf{n}}} = ikAP$
at $x = \pm l_x/2$; $y = \pm l_y/2$ (3)

where A is the normalized wall admittance of a “locally reacting” boundary and $\tilde{\mathbf{n}}$ is the outward normal.

The general solution for the pressure field in section I of the duct is given by, (the term $e^{i\omega t}$ is implicit throughout the paper)

$$P_I(x, y, z) = A_{m_0 n_0} \Psi(K_{m_0} x) \Psi(K_{n_0} y) e^{-iK_{m_0 n_0} z} + \sum_{m=1}^{\infty} \sum_{n=1}^{\infty} \hat{B}_{mn} \Psi(K_m x) \Psi(K_n y) e^{iK_{mn} z} \quad (4)$$

where,

$$\begin{cases} \Psi(K_m x) = \frac{\cos(K_m x)}{\sin(K_m x)} \\ \Psi(K_n y) = \frac{\cos(K_n y)}{\sin(K_n y)} \end{cases} \quad (5)$$

are the eigenfunctions. A cosine function is used for the even modes and a sine function for the odd modes. The transverse wave numbers K_m and K_n are determined by the boundary condition (2) and are

$$\begin{cases} K_m = (m-1)\pi / l_x \\ K_n = (n-1)\pi / l_y \end{cases} \quad (6)$$

where l_x and l_y are the cross-sectional dimensions of the duct in the x and y direction respectively. ‘ m ’ and ‘ n ’ are integers different from zero.

The axial wave number is given by the following dispersion equation

$$K_{mn}^2 = k^2 - (K_m^2 + K_n^2) \quad (7)$$

The propagation of the waves in the axial direction is possible as long as the axial wave number $K_{mn}^2 > 0$. According to equation (7), this is true for

$$\omega > c_0 \sqrt{K_m^2 + K_n^2} = \omega_{mn}^c \quad (8)$$

Below this “cut-off” frequency ω_{mn}^c , the axial wave number K_{mn} becomes a purely imaginary number, and the propagation factors in equation (4) turn into $e^{-|K_{mn}z|}$; which means the amplitudes of these modes decay exponentially with axial distance from the source: they are “cut-off”. Notice that the mode (m_0, n_0) is just one particular mode over all possible (m, n) modes.

Now, let us consider the case of a treated duct: the general solution for the pressure field in Section II of the duct is (assuming that reflections from the end of the duct are neglected)

$$P_{II}(x, y, z) = \sum_{q=1}^{\infty} \sum_{p=1}^{\infty} \hat{A}_{qp} \hat{\Psi}(\hat{K}_q x) \hat{\Psi}(\hat{K}_p y) e^{-i \hat{K}_{qp} z} \quad (9)$$

where,

$$\begin{cases} \hat{\Psi}(\hat{K}_q x) = \frac{\cos(\hat{K}_q x)}{\sin(\hat{K}_q x)} \\ \hat{\Psi}(\hat{K}_p y) = \frac{\cos(\hat{K}_p y)}{\sin(\hat{K}_p y)} \end{cases} \quad (10)$$

are the complex eigenfunctions. The transverse wave numbers are determined by the boundary condition (3),

$$\begin{cases} \hat{K}_q = \hat{\mu}_q \pi / l_x \\ \hat{K}_p = \hat{\mu}_p \pi / l_y \end{cases} \quad (11)$$

and the axial wave number by the following dispersion equation

$$\hat{K}_{qp}^2 = k^2 - (\hat{K}_q^2 + \hat{K}_p^2) \quad (12)$$

where $\hat{\mu}_q$ and $\hat{\mu}_p$ are complex numbers. Note, in this case, the "cut-off notion" has no physical meaning. Assuming $\hat{K}_{qp} = (\alpha \pm i \beta) k$, α is the non-dimensional axial wave number and β is the damping factor of the mode. β should be positive for a mode propagating in $z > 0$ direction. This means that we should look for a solution to equation (12) that gives attenuation.

Solving equation (9) by the method of separation of variables and imposing the boundary conditions (3) leads to the following characteristic equations

$$\left(\hat{K}_e l_j / 2 \right) \tan \left(\hat{K}_e l_j / 2 \right) = \pm i k A l_j / 2 \quad (13)$$

where the term in tangent is used for even modes and the one with cotangent for odd modes. Indices 'e' and 'j' represent q or p and x or y respectively depending on the propagation direction.

The axial and transverse wave numbers were computed using a numerical scheme developed by Eversman [16, 17], where the characteristic equation is transformed into a first order non-linear differential equation. The differential equation is integrated by using a Runge-Kutta algorithm with appropriate initial values. The transverse wave numbers are then used to compute the axial wave number using equation (12).

2.2 Calculation of Transmitted Modal Coefficients

The pressure and acoustic velocity are related by the momentum equation

$$\nabla \bar{P} = -i k \rho c_0 \bar{V} \quad (14)$$

Using equations (4) and (9), the axial velocity in both sections (I and II) can be written as

$$\begin{cases} V_I(x, y, z) = (1/k \rho c_0) \left\{ A_{m_0 n_0} K_{m_0 n_0} e^{-i K_{m_0 n_0} z} \Psi(K_{m_0} x) \Psi(K_{n_0} y) - \sum_{m=1}^{\infty} \sum_{n=1}^{\infty} \hat{B}_{mn} K_{mn} e^{i K_{mn} z} \Psi(K_m x) \Psi(K_n y) \right\} \\ V_{II}(x, y, z) = (1/k \rho c_0) \sum_{q=1}^{\infty} \sum_{p=1}^{\infty} \hat{A}_{qp} \hat{K}_{qp} \hat{\Psi}(\hat{K}_q x) \hat{\Psi}(\hat{K}_p y) e^{-i \hat{K}_{qp} z} \end{cases} \quad (15)$$

The unknown amplitudes \hat{A}_{qp} and \hat{B}_{mn} in equations (4), (9) and (15) are determined from a system of linear equations obtained by applying continuity conditions: the pressures and axial velocities in the two sections of the duct must be equal at the junction ($z = 0$) of the lined and unlined sections.

$$\begin{cases} P_I(x, y, 0) = P_{II}(x, y, 0) \\ V_I(x, y, 0) = V_{II}(x, y, 0) \end{cases} \quad (16)$$

Thus, by substituting equations (4), (9) and (15) into (16) and using the orthogonality properties of the eigenfunctions, the following system for the transmitted modal coefficients is obtained

$$\sum_{q=1}^{\infty} \sum_{p=1}^{\infty} \hat{A}_{qp} \hat{I}_{m'q} \hat{J}_{n'p} (\hat{K}_{qp} + K_{m'n'}) = A_{m_0 n_0} \frac{(1+\delta_{m_0 1})(1+\delta_{n_0 1})}{2} \delta_{m_0 m'} \delta_{n_0 n'} (K_{m'n'} + K_{m_0 n_0}) \quad (17)$$

where δ is the Kronecker delta and

$$\hat{I}_{ij} = \frac{1}{l_x} \int_{-l_x/2}^{l_x/2} \Psi(K_i, x) \hat{\Psi}(\hat{K}_j, x) dx \quad (18)$$

$$\hat{J}_{ij} = \frac{1}{l_y} \int_{-l_y/2}^{l_y/2} \Psi(K_i, y) \hat{\Psi}(\hat{K}_j, y) dy \quad (19)$$

Equations (18) and (19) are solved analytically. The same process as described above leads to a system of equation, as in (17) for the reflected modal coefficients. The reflected modal coefficients are not discussed here, since the aim is to calculate the radiated sound field.

The system indices, m and n , vary from 1 to M_m and 1 to N_n respectively; while q, p vary from 1 to Q_q and 1 to P_p respectively after truncation. M_m and N_n are the total possible propagating modes along 'x' and 'y' in Section I. Therefore, we have $[Q_q * P_p]$ complex equations and $[Q_q * P_p]$ complex unknown which are the transmitted modal coefficients. The final linear system (17) could be re-written as,

$$[a] \cdot [X] = [b] \quad (20)$$

where,

$[a]$ complex vector which contains the modal transmitted coefficients to be determined,

$[X]$ complex matrix which depends on the modes (m, n) and on the eigenvalues of the system,

$[b]$ known vector which depends on the incident mode (m_0, n_0) and its amplitude $A_{m_0 n_0}$.

The final matrix $[X]$ is square and the dimension of the system is multiplied by 2 to account for the complex numbers, therefor the final matrix dimension are $[2 * Q_q * P_p, 2 * Q_q * P_p]$. Further, The truncation is performed at $Q_q = M_m + 2$ and $P_p = N_n + 2$, and has been checked when calculating all possible transmitted and reflected coefficients at the discontinuity junction for any incident mode (m_0, n_0) . It has been found that it's worthless and time consuming to consider a number of modes (generated in section II) greater than the limit chosen above. Finally, a numerical scheme, using LU decomposition algorithm with a matrix inversion, has been used to solve the final matrix system.

3. RADIATION FROM THE END OF THE DUCT

The radiated acoustic power from the duct is evaluated using

$$W = \int_{\varphi=0}^{2\pi} \int_{\theta=0}^{\pi/2} \frac{|P(M)|^2}{2 \rho c_0} R^2 \sin \theta \, d\theta \, d\varphi \quad (21)$$

where $P(M)$ is the complex acoustic pressure at a location M in space expressed in spherical coordinates, $M = (R, \theta, \varphi)$.

The acoustic pressure in equation (21) can be written in terms of surface velocity using the Rayleigh integral,

$$P(M) = \frac{i\omega \rho}{2\pi} \int_S V(x_0, y_0) \Big|_{z=L} \frac{e^{-ikh}}{h} dS \quad (22)$$

where h is the distance between the source location $M_0(x_0, y_0)$ and the receiver location M . The acoustic far-field hypothesis leads to the following approximations

$$\frac{1}{h} \approx \frac{1}{R} \quad \text{for the amplitude, and}$$

$$kh \approx kR - D_x x_0 - D_y y_0 \quad \text{for the phase}$$

where,

$$D_x = k \sin \theta \cos \varphi \quad (23)$$

$$D_y = k \sin \theta \sin \varphi \quad (24)$$

3.1 Rigid Duct

Equation (22) can be calculated analytically for each incident mode of a rigid duct. For a given mode (m_0, n_0) the fluctuation of the pressure can be written as, for an even-even mode excluding the fundamental mode $(m, n) = (1, 1)$:

$$|P(M)| = \frac{1}{2\pi R} |A_{m_0 n_0}| |4 K_{m_0 n_0} | D_x | | D_y | \left| \frac{\sin(D_x l_x / 2)}{K_{m_0}^2 - D_x^2} \right| \left| \frac{\sin(D_y l_y / 2)}{K_{n_0}^2 - D_y^2} \right| \quad (25)$$

The term $\sin(D_x l_x/2)$ is replaced by $\cos(D_x l_x/2)$ in the case of an odd mode (same thing for the y direction). In the particular case of the fundamental mode $(m, n) = (1, 1)$, the expression (25) becomes:

$$|P(M)| = \frac{|A_{11}|}{2\pi R} k l_x l_y \left| \frac{\sin(D_x l_x/2)}{(D_x l_x/2)} \right| \left| \frac{\sin(D_y l_y/2)}{(D_y l_y/2)} \right| \quad (26)$$

3.2 Lined Duct

The axial velocity component in integral (22) is complex

$$|\hat{P}(M)| = \frac{1}{2\pi R} \sum_{q=1}^{Q_q} \sum_{p=1}^{P_p} |\hat{A}_{qp}| \operatorname{Re}\{\hat{K}_{qp}\} e^{-2\operatorname{Im}\{\hat{K}_{qp}\}L} \times \left| \frac{D_x \sin(D_x l_x/2) \cos(\hat{K}_q l_x/2) - \hat{K}_q \cos(D_x l_x/2) \sin(\hat{K}_q l_x/2)}{\hat{K}_q^2 - D_x^2} \right| \times \left| \frac{D_y \sin(D_y l_y/2) \cos(\hat{K}_p l_y/2) - \hat{K}_p \cos(D_y l_y/2) \sin(\hat{K}_p l_y/2)}{\hat{K}_p^2 - D_y^2} \right| \quad (28)$$

Similar expressions can be obtained for the other cases by replacing the term $D_x \sin(D_x l_x/2) \cos(\hat{K}_q l_x/2)$ with $D_x \cos(D_x l_x/2) \sin(\hat{K}_q l_x/2)$ of equation (28), and $\hat{K}_q \cos(D_x l_x/2) \sin(\hat{K}_q l_x/2)$ with $\hat{K}_q \sin(D_x l_x/2) \cos(\hat{K}_q l_x/2)$ in the case of an odd mode (same thing apply for the modes in the y direction).

4. RESULTS

In the existing literature, the possibility of changing the radiation pattern by modifying the aperture field has received a little attention. While, the attenuation properties of acoustical lining have been extensively studied, its effect on the radiation pattern has been overlooked.

The validity of the present formulation for the radiated field is first discussed. For this, we have compared the present approximate radiated field from a simple duct contained within two parallel semi-infinite rigid plates with the exact Wiener-Hopf solution of Candel [18].

with acoustic treatment and is given by,

$$V(x_0, y_0) = (1/k \rho c_0) \sum_{q=1}^{Q_q} \sum_{p=1}^{P_p} \hat{A}_{qp} \hat{K}_{qp} \hat{\Psi}(\hat{K}_q x_0) \hat{\Psi}(\hat{K}_p y_0) e^{-i \hat{K}_{qp} L} \quad (27)$$

By replacing (27) into (22) and calculating the integral analytically, we obtain the following expression for the fluctuating pressure:

4.1 Validation

Consider now the duct, shown in Figure 2, formed by two semi-infinite parallel plates. The acoustic pressure in the far-field is given by the Rayleigh Integral which is written as follows for the 2D case,

$$P(M) = i \omega \rho \int_l V(x_0) \Big|_{z=0} \frac{e^{-ikr}}{\sqrt{2\pi r}} dl \quad (29)$$

Following the same process as described above, the expressions of the acoustic pressure in the far field are given below

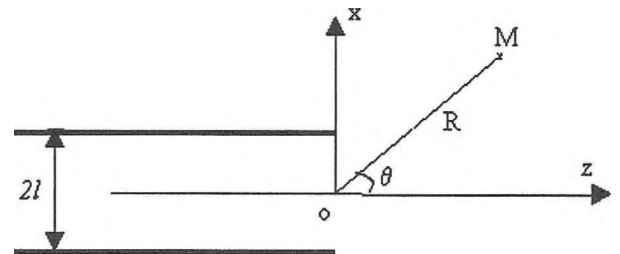


Figure 2. Geometry of the radiated problem for a duct formed by two semi-infinite rigid plates.

- Even modes (different from zero):

$$P(M) = \sqrt{\frac{2}{\pi r}} |A_{m_0}| \sqrt{1 - (K_{m_0}/k)^2} \left| \frac{\sin \theta \sin(kl \sin \theta)}{(K_{m_0}/k)^2 - \sin^2 \theta} \right| \quad (30)$$

- Odd modes:

$$P(M) = \sqrt{\frac{2}{\pi r}} |A_{m_0}| \sqrt{1 - (K_{m_0}/k)^2} \left| \frac{\sin \theta \cos(kl \sin \theta)}{(K_{m_0}/k)^2 - \sin^2 \theta} \right| \quad (31)$$

- Fundamental mode:

$$P(M) = \sqrt{\frac{2}{\pi r}} |A_{m_0}| kl \left| \frac{\sin(kl \sin \theta)}{(kl \sin \theta)} \right| \quad (32)$$

where,

$|A_{m_0}|$ is the amplitude of the incident mode m_0 and K_{m_0} is its transverse wave number. The radiation field for multiple values of $k * l$ (reduced frequency) was calculated with the same mode number $m_0 = 2$ (incident mode) of Candel [18].

The radiation patterns for a duct formed by two semi-infinite parallel rigid plates are shown in Figure 3. The radiation pattern shows a larger number of lobes, a greater peak pressure, and angular distribution displaced towards the duct axis with increasing frequency. Most importantly, the approximate solution, represented on the right, agrees well with the exact solution, represented on the left, by the Wiener-Hopf technique. Even at high frequency, the agreement is good even though there is less radiation behind the duct aperture. Moreover, the direction of the main lobe remains unchanged in both cases and with the same sound pressure level.

4.2 Examples

The method described in section 3 leads to a simple relation to calculate the radiated far field from any rectangular duct. It also provides a useful tool for analytical study of the influence of lined duct wall on the radiation pattern.

The liners considered in this example are absorbers made of fibrous materials backed by a hard surface. The liners are assumed to be locally reacting. For a given flow resistivity σ , liner thickness d and frequency f , the impedance of the liner is determined by the empirical formulae given by Delany and Bazley [19]. The principal formula is:

$$Z = -i Z_c \cot(K_c d) \quad (33)$$

where,

$$Z_c = \rho c_0 \left[1 + 0.0571 X^{-.754} - i 0.087 X^{-.732} \right] \quad (34)$$

$$K_c = k \left[1 + 0.0978 X^{-.700} - i 0.189 X^{-.595} \right] \quad (35)$$

Z_c is the characteristic impedance of the material, K_c its wave number and $X = \rho f / \sigma$ a non-dimensional parameter. The admittance of the liner is $A = \rho c_0 / Z$

4.3 Discussion

Directivity patterns for lined ducts are shown in Figures 4 through 10, for liner thickness of 100 mm and fill density of 25 kg/m³. The treatment length, L , is 1 m and the acoustic far field pressure is calculated at a distance (R) of 10 m from the opening.

In Figures 4(a), 5(a), 6(a) and 7(a) the radiation patterns of the fundamental mode (1,1) are shown for the case of a rectangular rigid duct at different frequencies given in Table 1. The figures show one main lobe presenting a maximum along the duct axis which is a characteristic for that mode, and two or several side lobes depending on the frequency parameters. The same observation as described in section 4.1 can be made here about the lateral lobes: when the frequency increase, the radiation pattern shows a larger number of lobes, a greater peak pressure, and an angular distribution is displaced towards the duct axis.

Figures 4(b), 5(b), 6(b) and 7(b) show the effect of the liner on the directivity patterns in the case of a lined duct. It is seen that the radiation to the lateral sides is strongly reduced while the main lobe becomes more wider.

The results for a higher order incident mode (2,2), are shown in Figure 8 for $kl_x/2 \approx 5.5$; $kl_y/2 \approx 3.5$ and in Figure 9 for $kl_x/2 \approx 22$; $kl_y/2 \approx 14$. The rigid duct case is represented in Figures 8(a), 9(a) and the lined case in Figures 8(b), 9(b). In the rigid case, the sound pressure level at the duct axis is zero and the directivity is stronger in the lateral sides with 4 main lobes. The effects of the acoustic treatment on the radiation remain as described above with a weak radiation in the lateral sides.

Finally, the incident mode (4,3) is shown in Figures 10(a) and 10(b) for the rigid case and the lined case respectively at frequency ($kl_x/2 \approx 22$; $kl_y/2 \approx 14$). The same observations are evident.

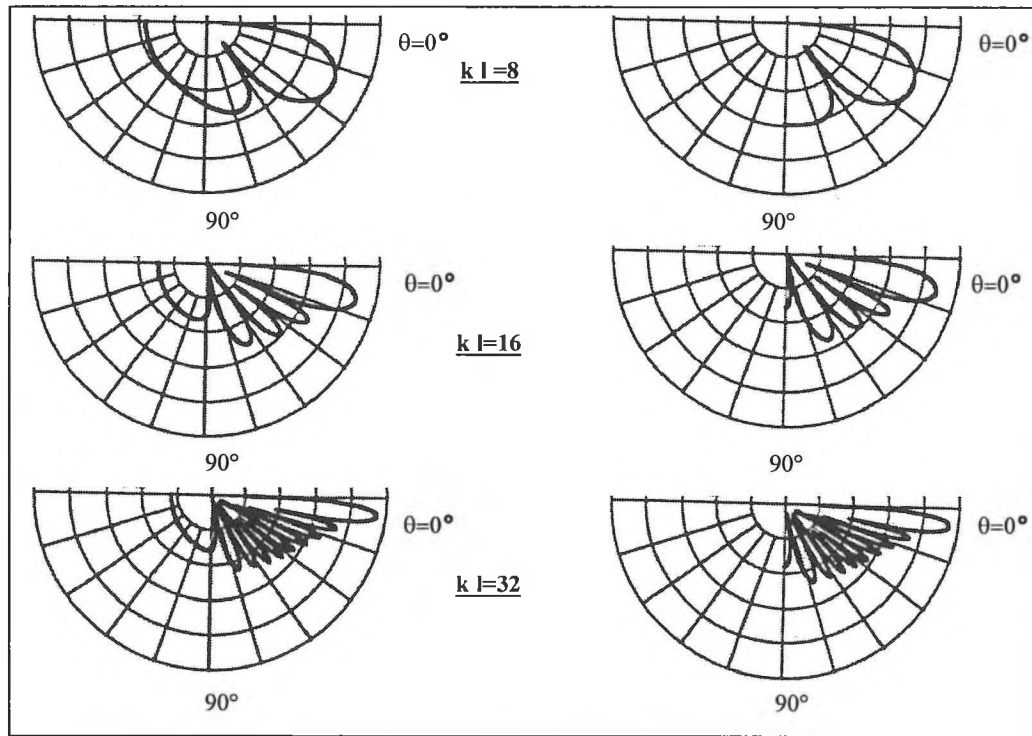


Figure 3. Radiation patterns for a duct formed by two semi-infinite parallel rigid plates. The exact Wiener-Hopf solution (by Candel [18]) is on the left; the approximate solution is on the right for different $k l$ and mode $m_0 = 2$ (scale: 10 dB per graduation).

Figure no.	Incident mode	Adimensional frequency parameter ($k l_x / 2; k l_y / 2$)	Normalized Admittance	Total possible modes	Possible modes in X direction	Possible modes in Y direction
4	(1,1)	(5.5; 3.5)	(1.15-i 0.53)	10	4	3
5	(1,1)	(11; 7)	(1.48-i 0.3)	31	7	5
6	(1,1)	(22; 14)	(1.1-i 0.25)	114	14	10
7	(1,1)	(55; 36)	(1.09-i 0.15)	668	35	24
8	(2,2)	(11; 7)	(1.48-i 0.3)	31	7	5
9	(2,2)	(22; 14)	(1.1-i 0.25)	114	14	10
10	(4,3)	(22; 14)	(1.1-i 0.25)	114	14	10

Table 1. Description of the parameters of Figures 4 to 10.

5. CONCLUSIONS

The radiation from a lined duct with finite length treatment was evaluated using analytical/numerical schemes. It was seen that the presence of an acoustic liner inside a duct significantly reduces the side radiation from the open end of the duct. The absorbing walls focus the acoustic energy towards the center axis of the duct. While, near the walls, the energy is absorbed and hence the pressure oscillations are small. The amplitude of the pressure field in the aperture is decreased towards the edges. Such a decrease is equivalent to a reduction of the aperture area and would

result in a broader main lobe in the radiation pattern and thus a lower directionality. However, the decreases in the amplitude of the pressure also produce a large reduction in the side lobe amplitudes. For the fundamental mode, the maximum of the radiated sound is reached at the duct axis as expected.

Finally, the analytical expressions developed here provide a useful tool to study the influence of a lined duct wall on the radiation pattern. It also allows the possibility of changing the radiation pattern by modifying the aperture field.

6. REFERENCES

- [1] J.S. Rayleigh, "The Theory of Sound" Dover Publication Inc. (1945).
- [2] H. Levine and J. Schwinger, "On the radiation of sound from an unflanged circular pipe", Physical Revue (1948), Vol. 73(4), pp 383-406.
- [3] B. Noble, "Methods based on the Wiener-Hopf technique", Pergamon Press, Oxford (1958).
- [4] J.M. Tyler & T.G. Sofrin, "Axial flow compressor noise studies", SAE Trans. (1962), vol. 70, pp 309-332.
- [5] C.L. Morfey, "A note on the radiation efficiency of acoustic duct modes", J. Sound and Vibration (1969), Vol. 9(3), pp. 367-372.
- [6] G.F. Homicz and J.A. Lordi, "A note on the radiative directivity patterns of duct acoustic modes", J. Sound and Vibration (1975), Vol. 41(3), pp. 283-290.
- [7] W.E. Zorumski, "Generalized radiation impedance and reflection coefficients of circular and annular ducts", J. Acoust. Society of America (1973), Vol. 54(6).
- [8] D.L. Lansing and W.E. Zorumski, "Effects of wall admittance changes on duct transmission and radiation of sound", J. Sound and Vib. (1973), Vol. 27(1), pp. 85-100.
- [9] W. Koch, "Radiation of sound from a two-dimensional acoustically lined duct", J. Sound and Vibration (1977), Vol. 55(2), pp. 255-274.
- [10] G.W Johnston and K. Ogimoto, "Sound radiation from a finite length unflanged circular duct with uniform axial flow", J. Acoust. Society of America (1980), Vol. 68(6).
- [11] S.M. Candel, "Acoustic radiation from the end of a two-dimensional duct, effects of uniform flow and duct lining", J. Sound and Vibration (1973), Vol. 28(1), pp. 1-13.
- [12] Y. Kagawa et al., "Finite element approach to acoustic transmission-radiation systems and application to horn and silencer design", J. Sound and Vibration (1980), Vol. 69(2), pp. 207-228.
- [13] T.L. Wu and L. Lee, "A direct boundary integral formulation for acoustic radiation in a subsonic uniform flow", J. Sound and Vibration (1994), Vol. 175(1), pp. 51-63.
- [14] M.A. Hamdi, "Formulation variationnelle par équations intégrales pour le calcul de champ linéaires proches et lointains", Thèse de Doctorat d'état (1982), Université Technologique de compiégne - France.
- [15] M.A. Hamdi and J.M. Ville, "Sound radiation from ducts: theory and experiment", J. Sound and Vibration (1986), Vol. 107(2), pp. 231-242.
- [16] W. Eversman, "Computation of axial and transverse waves numbers for uniform two-dimensional ducts with flow using a numerical integration scheme", J. Sound and Vibration (1975), vol. 41(2), pp. 252-255.
- [17] W. Eversman, "Initial values for the integration scheme to compute the eigenvalues for propagation in ducts", J. Sound and Vibration (1977), Vol. 50(1), pp. 159-162.
- [18] S.M. Candel, "Acoustic radiation from a two dimensional duct. Effects of uniform flow and duct lining", Ph.D dissertation (1972), Chapter V, California Institute of Technology.
- [19] M.E. Delany and E.N. Bazley, "Acoustical properties of fibrous absorbent materials", Applied Acoustics (1970), Vol. 3, pp. 105-116.

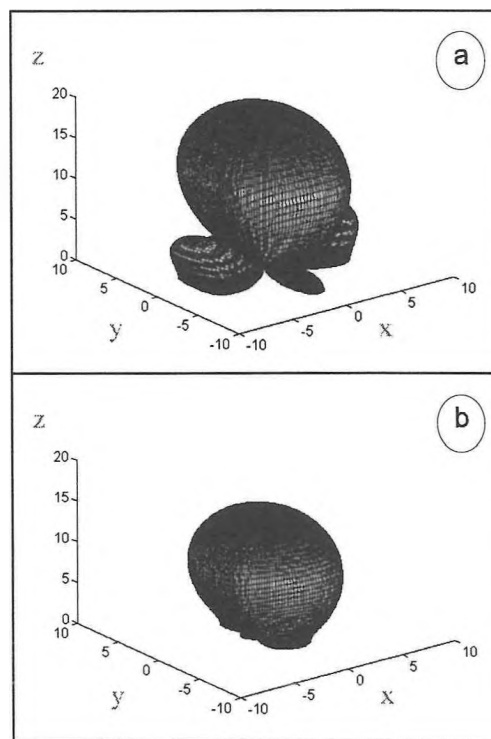


Figure 4. Directivity Patterns for mode incident (1,1), Adimensional frequency parameter ($k l_x/2$; $k l_y/2$)=(5.5; 3.5). (a) rigid case, (b) treated case. Normalized acoustic admittance=(1.15 - i .53).

x axis scale is $|P(M)| \sin \theta \cos \varphi$; y axis scale is $|P(M)| \sin \theta \sin \varphi$ and z axis scale is $|P(M)| \cos \theta$

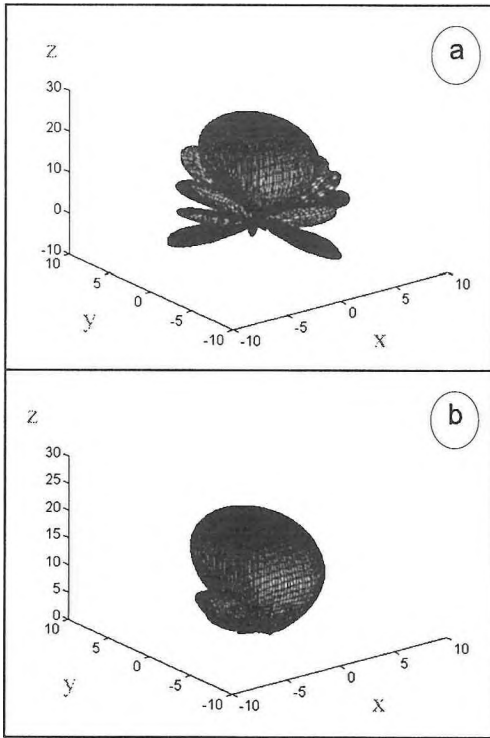


Figure 5. Directivity Patterns for mode incident (1,1), Adimensional frequency parameter $(k l_x/2; k l_y/2)=(11; 7)$. (a) rigid case, (b) treated case. Normalized acoustic admittance= $(1.48 - i .3)$.

x axis scale is $|P(M)| \sin \theta \cos \varphi$; y axis scale is $|P(M)| \sin \theta \sin \varphi$

and z axis scale is $|P(M)| \cos \theta$

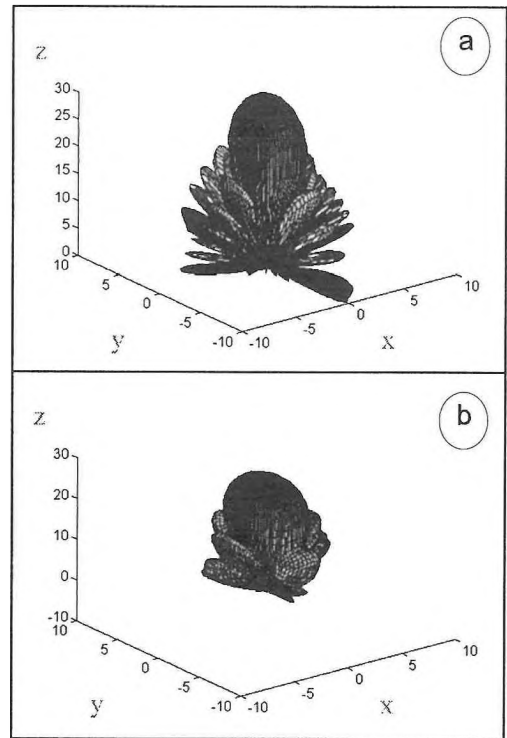


Figure 6. Directivity Patterns for mode incident (1,1), Adimensional frequency parameter $(k l_x/2; k l_y/2)=(22; 14)$. (a) rigid case, (b) treated case. Normalized acoustic admittance= $(1.1 - i .25)$.

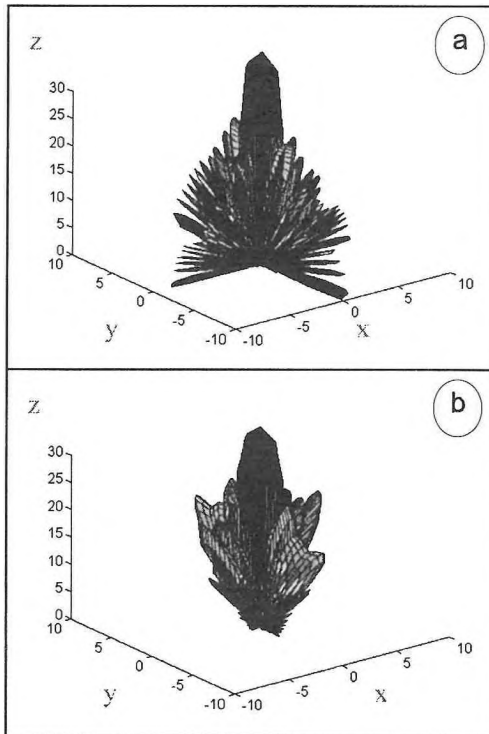


Figure 7. Directivity Patterns for mode incident (1,1), Adimensional frequency parameter $(k l_x/2; k l_y/2)=(55; 36)$. (a) rigid case, (b) treated case. Normalized acoustic admittance= $(1.09 - i .15)$.

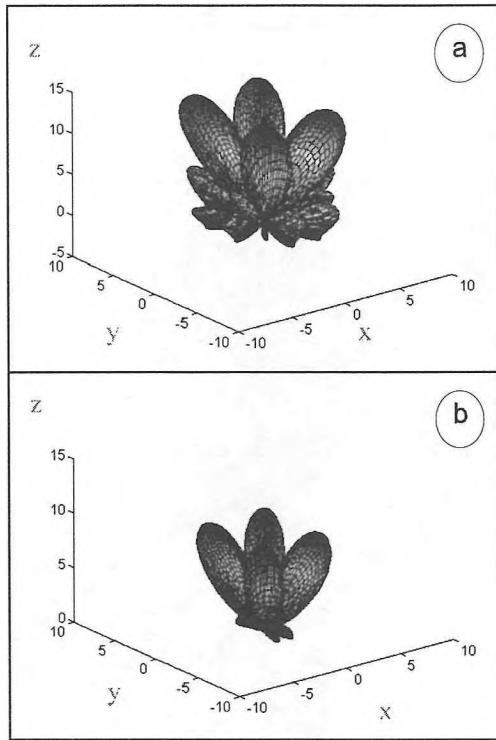


Figure 8. Directivity Patterns for mode incident (2,2), Adimensional frequency parameter $(k l_x/2; k l_y/2)=(11; 7)$. (a) rigid case, (b) treated case. Normalized acoustic admittance $= (1.48 - i .3)$.

x axis scale is $|P(M)| \sin \theta \cos \varphi$; y axis scale is $|P(M)| \sin \theta \sin \varphi$
and z axis scale is $|P(M)| \cos \theta$

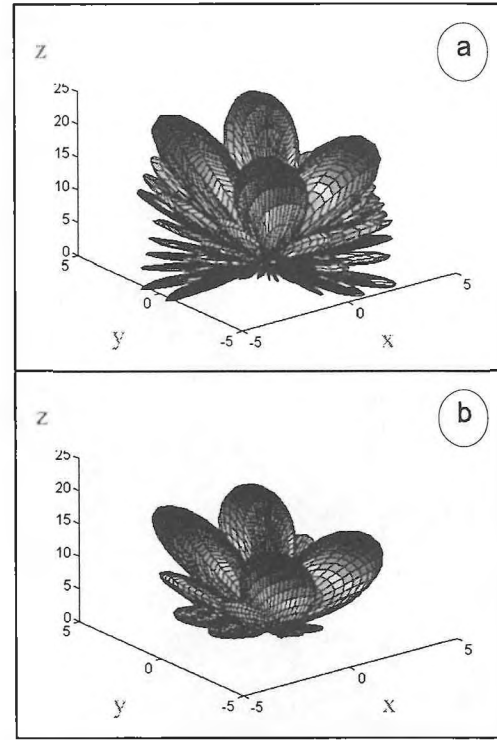


Figure 9. Directivity Patterns for mode incident (2,2), Adimensional frequency parameter $(k l_x/2; k l_y/2)=(22; 14)$. (a) rigid case, (b) treated case. Normalized acoustic admittance $= (1.1 - i .25)$.

x axis scale is $|P(M)| \sin \theta \cos \varphi$; y axis scale is $|P(M)| \sin \theta \sin \varphi$
and z axis scale is $|P(M)| \cos \theta$

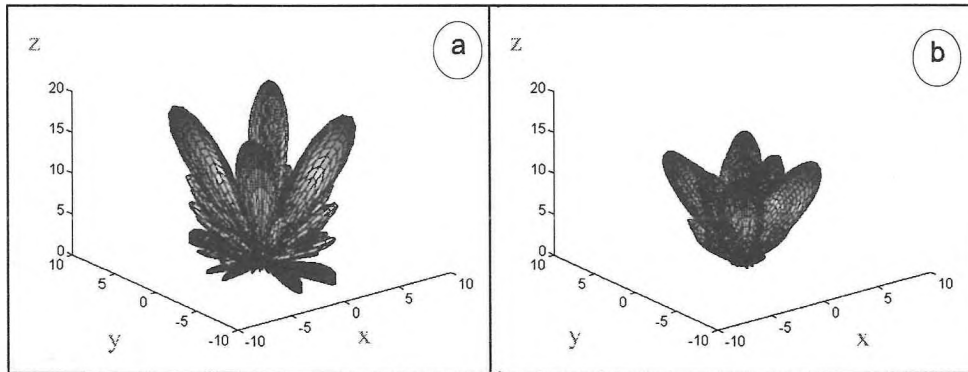


Figure 10. Directivity Patterns for mode incident (4,3), Adimensional frequency parameter $(k l_x/2; k l_y/2)=(22; 14)$. (a) rigid case, (b) treated case. Normalized acoustic admittance $= (1.1 - i .25)$.

x axis scale is $|P(M)| \sin \theta \cos \varphi$; y axis scale is $|P(M)| \sin \theta \sin \varphi$ and z axis scale is $|P(M)| \cos \theta$

SOUND INTENSITY MADE EASY



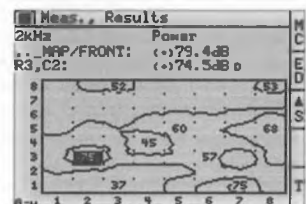
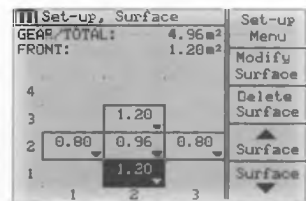
NOW IT'S A ONE-MAN JOB

Sound intensity in the palm of your hand. With the Hand-held Sound Intensity System it's easy for one person in the field to make a sound intensity measurement from initial scanning to final, on-the-spot results.

- ISO/ANSI sound power
- Noise source location
- Sound field analysis
- Building acoustics
- Automatic guidance and aural feedback

Everything you need to make a measurement, from a sound intensity analyzer to chalk for marking are included in the Hand-held Sound Intensity System, all neatly packed in a handy and robust carrying case.

Want to know more? Contact your local Brüel & Kjær sales representative today



98070

2260 INVESTIGATOR

Brüel & Kjær
2815 Colonnades Court • Norcross, GA 30071
TOLL FREE: (888) 788-1138 • Fax: (770) 447-2327 • FAX-ON-DEMAND: (800) 511-8602
e-mail: Bkinfo@SpectrisTech.com • Worldwide Web: www.BKhome.com

Brüel & Kjær